J Neurophysiol 103: 603–615, 2010.
First published December 2, 2009; doi:10.1152/jn.00510.2009.

Coding Characteristics of Spiking Local Interneurons During Imposed Limb Movements in the Locust

A. G. Vidal-Gadea,[1,*] X. J. Jing,[2,*] D. Simpson,[2] O. P. Dewhirst,[2] Y. Kondoh,[3] R. Allen,[2] and P. L. Newland[1]
[1]*School of Biological Sciences and* [2]*Institute for Sound and Vibration Research, University of Southampton, Southampton, United Kingdom; and* [3]*Honda R&D, Wako Research Center, Wako, Saitama, Japan*

Submitted 11 June 2009; accepted in final form 1 December 2009

Vidal-Gadea AG, Jing XJ, Simpson D, Dewhirst OP, Kondoh Y, Allen R, Newland PL. Coding characteristics of spiking local interneurons during imposed limb movements in the locust. *J Neurophysiol* 103: 603–615, 2010. First published December 2, 2009; doi:10.1152/jn.00510.2009. The performance of adaptive behavior relies on continuous sensory feedback to produce relevant modifications to central motor patterns. The femoral chordotonal organ (FeCO) of the legs of the desert locust monitors the movements of the tibia about the femoro-tibial joint. A ventral midline population of spiking local interneurons in the metathoracic ganglia integrates inputs from the FeCO. We used a Wiener kernel cross-correlation method combined with a Gaussian white noise stimulation of the FeCO to completely characterize and model the output dynamics of the ventral midline population of interneurons. A wide range of responses were observed, and interneurons could be classified into three broad groups that received excitatory and inhibitory or principally inhibitory or excitatory synaptic inputs from the FeCO. Interneurons that received mixed inputs also had the greatest linear responses but primarily responded to extension of the tibia and were mostly sensitive to stimulus velocity. Interneurons that received principally inhibitory inputs were sensitive to extension and to joint position. A small group of interneurons received purely excitatory synaptic inputs and were also sensitive to tibial extension. In addition to capturing the linear and nonlinear dynamics of this population of interneurons, first- and second-order Wiener kernels revealed that the dynamics of the interneurons in the population were graded and formed a spectrum of responses whereby the activity of many cells appeared to be required to adequately describe a particular stimulus characteristic, typical of population coding.

INTRODUCTION

Designing an artificial-limb control system inspired by biological control systems is a major challenge even when based on the simplest of animals since we know little of the huge integrative task performed by neuronal networks that control the limbs. How do the relatively small numbers of neurons in the insect CNS achieve the high degree of versatility of movement and similar precision as higher animals? To begin to understand this, we need to know in detail how sensory signals are processed in the CNS and what roles are played by different interneurons in the networks. Few studies, however, have systematically analyzed the coding properties of the interneurons, and those that have ignored their nonlinear properties.

The importance of precise control of limb movements is such that organisms as diverse as vertebrates and arthropods are endowed with a plethora of mechanoreceptors that monitor their limb movements. Vertebrates are equipped with muscle spindles (Mathews and Stein 1969), Golgi receptor organs (Mathews 1933), and stretch receptors (Sinclair 1981), while arthropods use bipolar cells (Hilton 1924; Rogosina 1928), campaniform sensilla (Pringle 1938a,b, 1940; Zill and Moran 1981), hair sensilla (Pringle 1938c), muscle receptor organs (Slifer and Finlayson 1956), joint receptors (Coillot and Boistel 1968), and chordotonal organs (Usherwood et al. 1968) that monitor muscle length, joint angle, velocity, and acceleration of their limbs (Bässler 1972a,b; Burrows and Horridge 1974; Field and Rind 1981; Full 1994; Gordon 1991; Gordon and Ghez 1991; Pearson 1993).

In the locust a proprioceptor in the hind leg, the femoral chordotonal organ (FeCO), consisting of ~90 sensory neurons (Matheson and Field 1990), monitors the movement of the tibia about the femoro-tibial joint (Bräunig 1985; Usherwood et al. 1968). The population of sensory neurons of the FeCO has an overlapping range of responses from encoding position to velocity and to acceleration (Kondoh et al. 1995) and is responsible for a resistance reflex that opposes the movement applied to the leg (Field and Burrows 1982). In locusts, in common with other insects, the FeCO afferents synapse directly onto spiking and nonspiking local interneurons and leg motor neurons (Burrows 1987a; Büschges 1989). Different sensory neurons respond to different qualities and ranges of stimuli (Kondoh et al. 1995), and these properties are thought to be translated onto their principal postsynaptic targets, the spiking local interneurons (Burrows 1988). However, it has been difficult to characterize populations of interneurons using standard ramp and sinusoidal stimuli, which only provide limited insight into the dynamic characteristics of the system.

Wiener kernel analysis using Gaussian white noise (GWN) as a stimulus enables a more complete and systematic characterization of a neural system by modeling its transfer characteristics (Marmarelis 2004; Marmarelis and Marmarelis 1978) and has been previously utilized to provide thorough characterizations of the properties of the locust FeCO proprioceptive afferents (Kondoh et al. 1995), the flexor (Newland and Kondoh 1997a) and extensor tibia motor neurons (Newland and Kondoh 1997b). The nonlinear models overcome the limitation of linear models, which always respond symmetrically to flexion and extension. Equally important, mathematical model descriptions allow prediction of responses of a characterized neuron to any given input, thus providing robust methods for comparison of neurons and network properties between animals (Marmarelis 2004).

Previous studies of the linear responses of a population of spiking interneurons located on the ventral ganglionic midline

* A. G. Vidal-Gadea and X. J. Jing contributed equally to this work.

Address for reprint requests and other correspondence: P. L. Newland, University of Southampton, B62/6041 Boldrewood Campus, Southampton SO16 7PX, UK (E-mail: P.L.Newland@soton.ac.uk).

established that they respond to the position of the tibia, and to the imposed direction, amplitude, and velocity of the motion (Burrows 1988). Since interneurons may, however, be involved in different aspects of sensory processing, studies of individual interneurons are insufficient to portray an accurate image of the tasks performed by the population and whether joint movement is encoded by the activity of single components in the population or the combined activity of many interneurons (known as population coding). To understand the role of the spiking local interneurons in the integration of sensory information and the modulation of behavior, it is therefore necessary to thoroughly quantify both their linear and nonlinear responses to sensory signals from the FeCO.

In this study we therefore used physiological and mathematical techniques to describe and model the dynamics of the synaptic activity of a population of spiking local interneurons in response to imposed limb movement about the femoro-tibial joint. The resulting mathematical models were used to test the responses of the interneurons to any arbitrary input and were tested to reveal how well the models fitted the actual responses.

METHODS

Adult male and female desert locusts, *Schistocerca gregaria* (Forskål), taken from our crowded colony were used for all experiments. Locusts were mounted ventral-side-uppermost in modelling clay. A hind leg was rotated 90° and fixed with the anterior face uppermost at a femoro-tibial angle of 60°, an angle in the middle of the linear range of movement of the FeCO apodeme (Field and Burrows 1982). The apodeme was then exposed by opening a window of cuticle in the distal anterior femur (Fig. 1, *A* and *B*) (see Burrows 1987b for a more detailed description), grasped between the tips of fine forceps attached to a vibrator (Ling Altec 101) and cut distal to the forceps.

To gain access to the CNS, a small window was cut in the ventral thorax to expose the meso- and metathoracic ganglia that were then supported on a wax-coated silver platform. The thorax was superfused with a constant flow of saline at 24°C. The posterior connectives of the metathoracic ganglion were cut while the anterior connectives and lateral

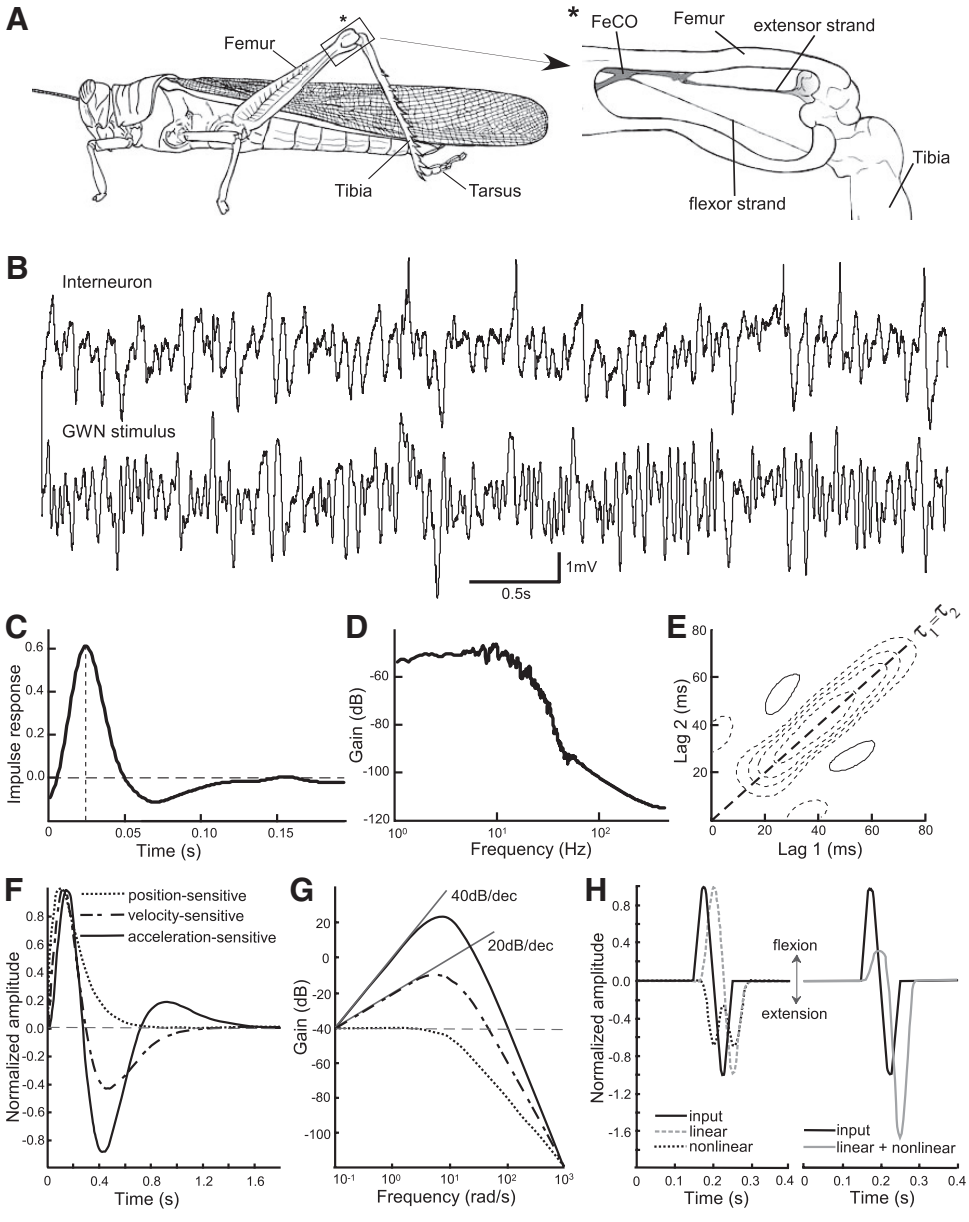

FIG. 1. The femoral chordotonal organ (FeCO) of a locust (*A*) was stimulated with Gaussian white noise (GWN) while recording the membrane potentials of spiking local interneurons (*B*). The 1st- and 2nd-order Wiener kernels were estimated by cross-correlation. The 1st-order kernel (*C*) shows how linearly an interneuron responds to the stimulus, and the frequency-response (*D*) demonstrates these corresponding properties in the frequency domain. The 2nd-order kernel (*E*) shows the nonlinear response properties of the interneuron. —, peaks; - - -, troughs. In this example, the monophasic 1st-order kernel with flat gain shows the interneuron is position-sensitive, the large valley along the diagonal in the 2nd-order kernel [where τ_1 (lag 1) = τ_2 (lag 2)] indicates hyperpolarisation in response to both flexion and extension, which is added to the 1st-order response. Illustrative 1st-order kernels (*F*) and gain curves (*G*) show how the stimulus qualities to which interneurons can be most sensitive affect the shape of these curves. *H*: typical responses of an interneuron to a sinusoidal input based on linear and nonlinear models (*left* showing u, $\hat{y}_1$ and $\hat{y}_2$) and on a combination of both models (*right*). The linear component in the response gives equal sensitivity both to flexion and extension with excitation during flexion and inhibition during extension; whereas the nonlinear component in the response is observed to be inhibitive both to the flexion and extension. Taken together (*right*), the neuron response is more sensitive (inhibited) to extension and only weakly excited during flexion.

nerve remained intact. The sheath of the ganglion was treated directly with protease (Sigma type XIV) for 1 min before recording. Microelectrodes filled with potassium acetate and with DC resistances of 50–80 MΩ were driven through the sheath and into the somata of the spiking local interneurons of the ventral midline group (Newland and Kondoh 1997a). Intracellular recordings were made using an Axoclamp 2A amplifier (Axon Instruments) and results based on successful recordings of 29 interneurons from 15 animals. All 29 interneurons had clear first-order kernels; however, 2 of the 29 (group 3) interneurons had noisy second-order kernels and were omitted from analyses.

FeCO stimulation

The forceps holding the chordotonal organ apodeme were moved with a GWN signal produced by filtering a pseudorandom binary sequence generated by a random binary generator (CG-742, NF Circuit Design Block) that was band-limited from DC to 200 Hz with low-pass filters (SR-4BL, NF Circuit Design Block) with a decay of 24 dB/octave. This generated a GWN signal with a flat power spectrum ≤200 Hz and a Gaussian probability density function. To move the FeCO apodeme, the source signal was then further filtered to generate white-noise signals with a cut-off frequency (f_c) of 27 Hz. Stimulus and evoked responses of the interneurons were stored on magnetic tape using a PCM-DAT data recorder (RD-101T, TEAC). The data were then imported into Matlab (Mathworks, Cambridge, UK) where it was analyzed using in-house software.

In the context of this study, we defined the input signal as the GWN stimulus described in the preceding text (0–27 Hz) and the output signal as the resulting synaptic potentials in the interneuron; from a physiological point of view, the latter can be considered the physiological input stimulus to the spiking interneuron.

Data analysis

The Wiener kernel method is robust to additive and uncorrelated white noise (Schetzen 1981) and convenient in terms of its simplicity in computation and integration making it an ideal method for modeling the input-output relationships of neuronal control systems. It is also a powerful method for examining, qualitatively and quantitatively, a system's dynamic response properties in cases where the output depends mostly on recent input (fading memory systems) (Boyd and Chua 1985). If the input signal is GWN (normally distributed amplitude, uncorrelated samples with mean value of zero), the Wiener method allows the output signal to be decomposed into a series of uncorrelated (orthogonal) components. These are constructed from Wiener kernels (Fig. 1, *C* and *E*), applied to the input signal. In this study, the input signal [denoted by $u(t)$] is the GWN that modulates the change in length of the FeCO apodeme, and the system output [denoted by $y(t)$] is the response (synaptic potential) recorded from the spiking local interneurons (Fig. 1, *A–D*). For a second-order Wiener model, this output is predicted by

$$\hat{y}(t) = \mathrm{E}\{y(t)\} + \hat{y}_1(t) + \hat{y}_2(t) \tag{1}$$

where $\mathrm{E}\{\cdot\}$ refers to the expected (or mean) value. Thus $\mathrm{E}\{y(t)\}$ is an offset, given by the mean value of the output, and $\hat{y}_1(t)$ and $\hat{y}_2(t)$ are the first- and second-order responses. The accuracy of the prediction performance can be evaluated by the following fitting function

$$\text{fit} = 1 - \|y(t) - \hat{y}(t)\|/\|y(t)\| \tag{2}$$

where $\|\cdot\|$ refers to the Euclidean norm (mean square value). A fit = 1 indicates that the model predicts the output perfectly, and fit = 0 very poor (or no) fit.

The fitting function can be computed separately for the linear model [without $\hat{y}_2(t)$ in *Eq. 1*] and the second-order model as given in *Eq. 1*. Higher model orders may also be used to fit more complex systems but lead to greatly increased computational load; in the current work, we will only use first- and second-order models.

In *Eq. 1*, $\hat{y}_1(t)$ is the estimation of the linear component in the system output response, which is computed by

$$\hat{y}_1(n) = \sum_{\tau=0}^{N_1} \hat{h}_1(\tau)u(n-\tau) \tag{3A}$$

where, $\hat{h}_i(\tau)$ is the estimated first-order Wiener kernel. The number of coefficients in the kernel ($N_1 + 1$) relates to the "memory" of the system. Thus for the first-order kernel

$$\hat{h}_1(\tau) = \frac{1}{P}\mathrm{E}\{y(t)u(t-\tau)\} \tag{3B}$$

where $\mathrm{E}\{\cdot\}$ represents the mean (or expected) value of the corresponding time series [i.e., the cross-correlation between $y(t)$ and $u(t-\tau)$]; $u(t-\tau)$ is the delayed version of the input; P is the power level ($\mathrm{E}\{u(t)^2\}$) of the input.

Since $u(t)$ is GWN, $\hat{h}_1(\tau)$ can be regarded as the best linear approximation of the system impulse response, and thus *Eq. 3A* represents the best approximation to the underlying linear dynamics between the system input and output. The first-order kernel $\hat{h}_1(\tau)$ can be used to study the linear dynamics of the interneurons. One feature of these linear responses is that they are always symmetrical: if flexion provokes excitation, then extension leads to inhibition and vice versa.

The first-order kernel alone cannot model the characteristics of neuronal responses such as differing sensitivity to flexion and extension. To overcome this, second-order systems include a wider range of system behaviors:

$$\hat{y}_2(n) = \sum_{\tau=0}^{N_2}\sum_{\tau=0}^{N_2}\hat{h}_2(\tau_1,\tau_2)u(n-\tau_1)u(n-\tau_2) - P\sum_{\tau=0}^{N_2}\hat{h}_2(\tau,\tau) \tag{4A}$$

The second-order kernel $\hat{h}_2(\tau_1,\tau_2)$ can be computed from

$$\hat{h}_2(\tau_1,\tau_2) = \frac{1}{2P^2}\mathrm{E}\{y(t) - \mathrm{E}\{y(t)\}\}u(t-\tau_1)u(t-\tau_2) \tag{4B}$$

provided that the input is GWN. In the current work, the kernels were estimated using the Lee-Schetzen method modified for band-limited input signals (Lee and Schetzen 1965; Schetzen 1981), which is computationally efficient. An example of input and output signals as well as first- and second-order kernels is plotted in Fig. 1. In these graphs, a movement into flexion is given as a deflection in the positive direction (upward), and on the output, a positive deflection shows depolarization and a negative deflection hyperpolarization. On the two-dimensional plots for the second-order kernels, depolarization (—) and hyperpolarization (- - -) are shown. While the methods for estimating the models are well defined, interpreting the results can be challenging. This will be addressed in the next section.

Interpreting the linear and nonlinear dynamics

The sensitivity of an interneuron's response to position, velocity, and acceleration are crucial to understanding how interneurons encode information related to movement of the tibia about the femoro-tibial joint. These can be revealed by the impulse and frequency response of the system (Fig. 1, *C* and *D*), i.e., the first-order kernels. To facilitate the interpretation, the first-order kernels for an ideal position, velocity, and acceleration-dependent system (but limited to frequencies below a cut-off at 27 Hz) are shown (Fig. 1*F*) together with the corresponding frequency responses (*G*). Thus a monophasic time-domain kernel with a flat frequency response (up to the cut-off frequency) indicates a (mainly) position-sensitive system. A biphasic kernel is indicative of

velocity sensitivity and shows a frequency response with a linear increase (20 dB/dec, Fig. 1*G*). An acceleration sensitive interneuron has a triphasic first-order kernel (and an even greater slope in its frequency response (40 dB/dec; Fig. 1*G*).

While the first-order kernel would be sufficient to describe the dynamic characteristics of an interneuron if it behaved linearly, in practice most interneurons have a nonlinear component. The second-order kernel describes some nonlinear dynamics of the interneuron and can reveal how it integrates stimuli over time (Fig. 1*E*). For example, the shape, size, and position of the dominant peak in a second-order kernel shows how the present activity of an interneuron is influenced by inputs occurring at two previous points in time ($t - \tau_1$ and $t - \tau_2$). The dominant peak in the second-order kernel for the interneuron in Fig. 1*E* is narrow and elongated along the diagonal (where $\tau_1 = \tau_2$) and reaches its maximum 40 ms after the stimulus onset.

Combining (by addition, see *Eq. 1*) the first- and second-order models can reveal how the linear and nonlinear characteristics of the interneuron interact in the production of a response. In the example of the interneuron in Fig. 1*H,* the positive first-order kernel combines with the negative dominant peak in the second-order kernel to reveal that this interneuron is strongly inhibited by extension and weakly excited by flexion of the tibia.

RESULTS

Effect of filtering spikes on first- and second-order kernels

Model-based analysis provided estimates of the first- and second-order kernels that were used to characterize interneuron responses to movement about the femoro-tibial joint. An example of one interneuron that was inhibited by FeCO stimulation illustrates many of the response dynamics of the population of interneurons as a whole (Fig. 2*Ai*). The first-order kernel of the synaptic response of an interneuron with no spikes is mainly monophasic (Fig. 2*Aii*), which indicates that this interneuron responded primarily to the position of the tibia about the femoro-tibial joint (cf. Fig. 1). The positive-going peak in the first-order kernel indicates that the response is excitatory in flexion and therefore inhibitory in extension. The valley on the diagonal of the second-order kernel is its largest feature and suggests that the interneuron is inhibited by both flexion and extension (Fig. 2*Aiv*). However, taking the two kernels together by adding their responses (*Eq. 1*) shows that an inhibitory response to extension alone is observed (as illustrated in Fig. 1*H*). An analysis of the interneuron's response in the frequency domain revealed that it had a relatively flat gain at low frequencies, which gradually declines >5 Hz (Fig. 2*Aiii*). Taken together these results indicate that the interneuron was position sensitive, had a low-passed response and with a major nonlinearity occurring during extension that enhanced the extension response, and depressed a flexion response; this represents a compressive (or rectification) nonlinearity.

Interneurons often produced spikes during FeCO stimulation with a mean of 5.25 ± 1.05 (SE) spike/s ($n = 29$) ranging from 0 to 21.6 spike/s. To determine if filtering action potentials prior to Wiener kernel analysis of synaptic responses had an impact on the response characteristics, we carried out the analysis with and without preprocessing. We found that the kernels were not greatly affected by spiking (Fig. 2*B*) either through low-pass filtering with a cut-off frequency at 90 Hz or truncation of each spike with replacement of these samples by linear interpolation of samples from either side of the spike (Fig. 2*C*). Based on these results, and similar results from other cases, further analysis used the raw recorded data without explicit spike-removal.

Analysis of synaptic inputs to the midline spiking local interneurons

Intracellular recordings from the midline spiking local interneurons during GWN stimulation revealed a range of responses following onset of stimulation (Fig. 3). Visual inspection of interneuron responses showed that most interneurons (15 of 29) received a barrage of inhibitory postsynaptic potentials (IPSPs) superimposed on a long-lasting hyperpolarizing potential, which in some interneurons completely suppressed the spontaneous burst of action potentials (Fig. 3*A*). A smaller group of interneu-

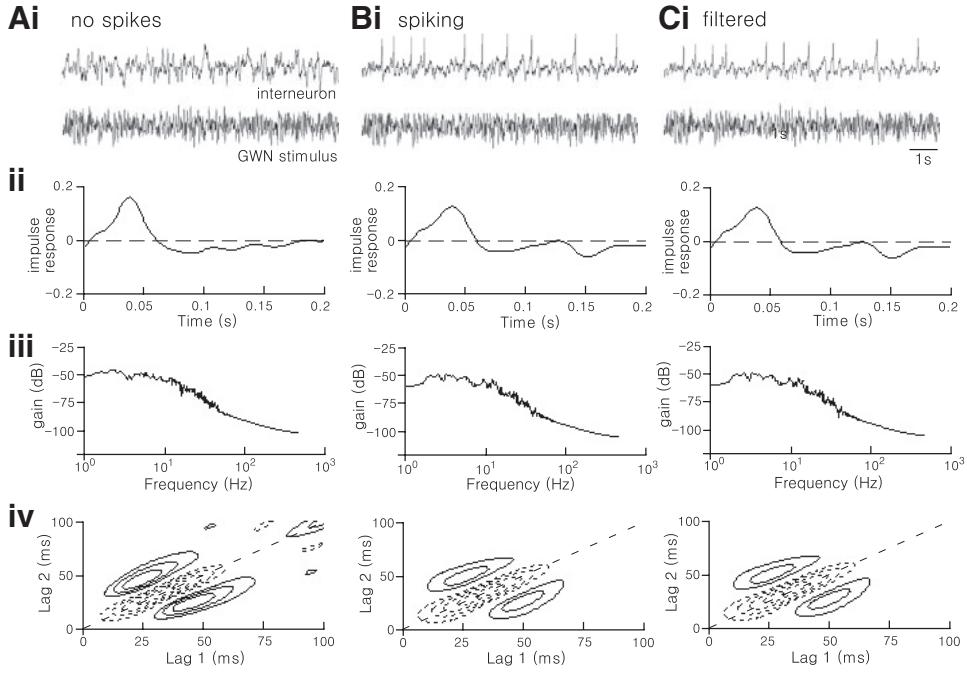

FIG. 2. Spike filtering does not affect the dynamic properties of the responses of an interneuron. *A*: the response (*i*), 1st-order kernel (*ii*), frequency response (*iii*), and 2nd-order kernels (*iv*) estimated from the response of an interneuron while it was not spiking and show that it is extension-sensitive. *B, i–iv*: analysis of the same interneuron during spiking at ~1 spike/s. The kernels estimated from the same interneuron at low firing rates show that the main output dynamic properties of the interneuron are similar to the synaptic component alone, and the frequency response remains unchanged. *C, i–iv*: analysis of the same dataset as in *B,* but with spikes truncated by linear interpolation of samples from either side of the spike. Note there is no major change in 1st-order kernel (*ii*), frequency response (*iii*), or 2nd-order kernel (*iv*) under these different spiking conditions.

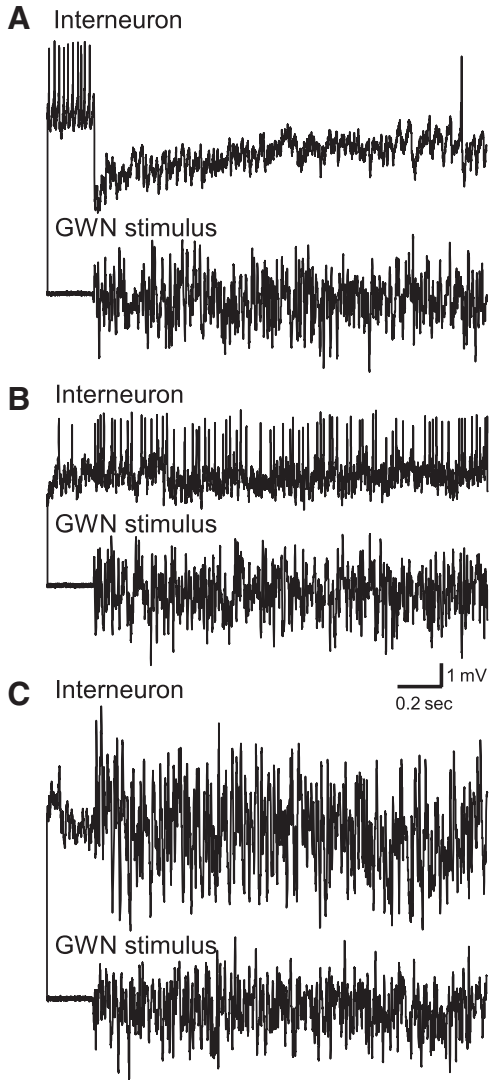

FIG. 3. Response properties of interneurons to GWN. Individual examples showing that stimulation of the FeCO led to interneurons receiving principally inhibitory inputs (*A*), principally excitatory inputs (*B*), or combined excitatory and inhibitory inputs (*C*).

rons (4 of 29) received purely excitatory input giving rise to an increase in the number of spikes evoked during stimulation (Fig. 3*B*) Finally, a third group of interneurons (10 of 29) received a combined input of EPSPs and IPSPs during FeCO stimulation (Fig. 3*C*).

Linear dynamics of individual interneurons

The kernels from the 29 interneurons show many similarities in shape and a wide range of peak times. In all cases, the frequency response was fairly flat up to ~27 Hz. To identify groups of responses in a quantitative manner, the response dynamics of all 29 interneurons were analyzed using a *K* means clustering algorithm (Hartigan and Wong 1979) applied to the frequency response (magnitude only) ≤30 Hz rather than using the first-order kernels that include noise from all frequencies (including frequencies above those used in stimulation, where estimates are less robust) and variable delays that are of little relevance in the current analysis. Cluster analysis was carried out in the frequency domain based on the slopes (0 and −30 dB/dec slopes, 5 and −10 dB/dec slopes, and 0 dB/dec slope, see in Fig. 4) to cluster kernels with respect to their sensitivity to position, velocity or acceleration. As Fig. 4 shows, there was overlap in the responses of groups 1 and 2. The kernels in group 1 (14 interneurons) were, however, principally monophasic with approximately flat frequency responses in the range 0–10 Hz and a decrease of −30 dB/dec >10 Hz, indicating that this group were position sensitive with a sharp low-pass filter characteristic. On the other hand, the interneurons in group 2 (11 interneurons) had a fast response time (reaching a peak value earlier), and the corresponding frequency responses indicate a 5 dB/dec increase <10 Hz and a −10 dB/dec decrease thereafter. The linear dynamics of the interneurons in group 2 were therefore more velocity- and acceleration-sensitive according to their frequency responses and responded with a short latency to the velocity and acceleration information within a stimulus. The time to peak of the first-order kernels showed that in general, the interneurons sensitive to velocity in group 2 respond faster to the FeCO stimulus compared with the interneurons in group 1. The average time to peak of the first-order kernels in group 2 was 18 ms, whereas the time to peak for the kernels in group 1 was 33 ms. Interneurons in group 3 contained responses that had negative monophasic first-order kernels with frequency responses with an approximately flat gain in the range 0–10 Hz indicating that they were mainly position sensitive (Fig. 4).

Dynamic properties of the second-order kernels

We used the second-order kernels to investigate the nonlinear dynamics of the spiking local interneurons in the three groups (Fig. 5). The system response is the sum of the first- and second-order responses. The interneurons in groups 1 and 2 (Fig. 5, *A* and *B*) had dominant negative peaks in their second-order kernels that when combined with the positive dominant peaks in their first-order kernel indicate that they were strongly inhibited by extension and only weakly excited by flexion. The converse of this was the case for interneurons in group 3 (Fig. 5*C*) that had dominant negative peaks in their first-order kernels and positive peaks in their second-order kernels, indicating that they were strongly excited by extension and weakly inhibited by flexion.

Within a particular group, the manner in which past inputs nonlinearly affected the interneuron response (as given by the kernels) were similar. For example, most interneurons in group 1 had negative dominant inhibitory peaks along the diagonal line ($\tau_1 = \tau_2$) with two smaller positive peaks closely beside (Fig. 5, *A* and *B*). We used the dominant-sensitive area to separate group 1 interneurons into two subgroups (Fig. 5*A, i* and *ii*). Interneurons in the first subgroup had kernels with a long inhibitory area on the diagonal with peaks at $\tau_1 = \tau_2 = 30$ ms (Fig. 5*Ai*). Interneurons of the second subgroup had circular inhibitory areas that peaked closer to the origin ($\tau_1 = \tau_2 = 20$ ms) and were smaller in size than the previous subgroup (Fig. 5*Aii*); these interneurons also had faster first-order responses. The kernels of the interneurons in the second subgroup 2 (Fig. 5*Aii*) therefore responded faster and were more sensitive to changes in the input compared with the first subgroup (*Ai*).

A similar trend was found in the velocity-sensitive (group 2) interneurons (Fig. 5*B, i* and *ii*). A comparison of the average of the dominant-sensitive areas showed that velocity-sensitive interneu-

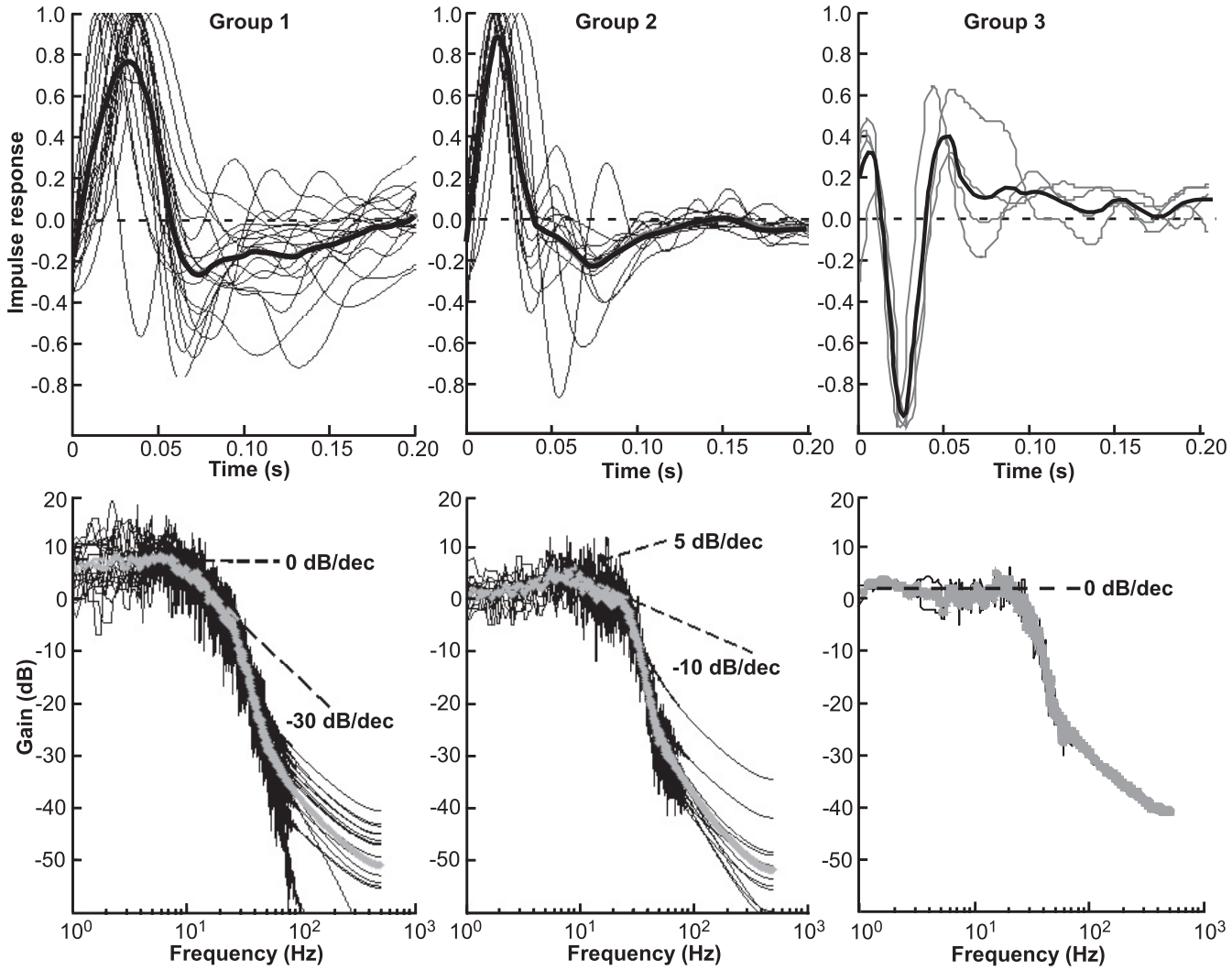

FIG. 4. First-order Wiener kernels for 29 interneurons (separated into 3 groups using K means cluster analysis). The impulse responses of the 1st-order kernels were normalized to a unit peak value. The monophasic kernels and flat frequency curves indicated that groups 1 and 3 were position sensitive (*left* and *right graphs,* respectively). Group 2 interneurons had biphasic kernels and positive slopes in the frequency response and were therefore more velocity sensitive (*middle graphs*).

rons had second-order kernels with dominant deflections which peaked closer to the origin and were therefore more sensitive and faster to respond to stimulus changes (which is typical of velocity-sensitive neurons). Group 3 interneurons (flexion/position sensitive) had fast peak times for the second-order kernels that were consistent with those for the first-order kernels.

Using Wiener kernel models to predict the response of a system to arbitrary stimuli

We evaluated the three groups defined by Wiener kernel analysis by analyzing the model predictions on stimuli specifically designed to provide intervals with a range of constant positions and velocities (Fig. 6). The plot shows typical results obtained from one recording in each of the three groups. For the linear kernels (Fig. 6*A*), groups 1 and 2 are seen to be excitatory during flexion and inhibitory during extension. Group 1 is mainly position sensitive and group 2 more velocity sensitive, as it shows the strongest response to a change in position. Group 3 is also mainly position sensitive but inhibited during flexion and excited during extension. As discussed previously, the linear response is symmetrical with the response to flexion always being simply the inverse of that to extension. For the sum of the first- and second-order kernels (as used to generate the nonlinear models—*Eq. 1*), the response becomes asymmetrical: for all groups there was greater sensitivity to extension than to flexion. For groups 1 and 2 (Fig. 6*B, i* and *ii*), there was inhibition during extension (with only a small excitatory response to flexion) and for group 3 (Fig. 6*Biii*), the inverse was found. These observations are consistent with the analysis of the first- and second-order kernels presented in the preceding text. Of the responses of all 29 interneurons, it is clear that no interneuron responded purely to position, velocity or acceleration, or purely flexion or extension but rather to a mixture of all these.

Validity of model predictions of the interneuronal responses

The accuracy of the computed Wiener kernel-based model (from *Eqs 1–4*) can be measured by the fit function defined in *Eq. 2*. The values of the fit functions for the linear and second-order models directly indicate to what extent an inter-

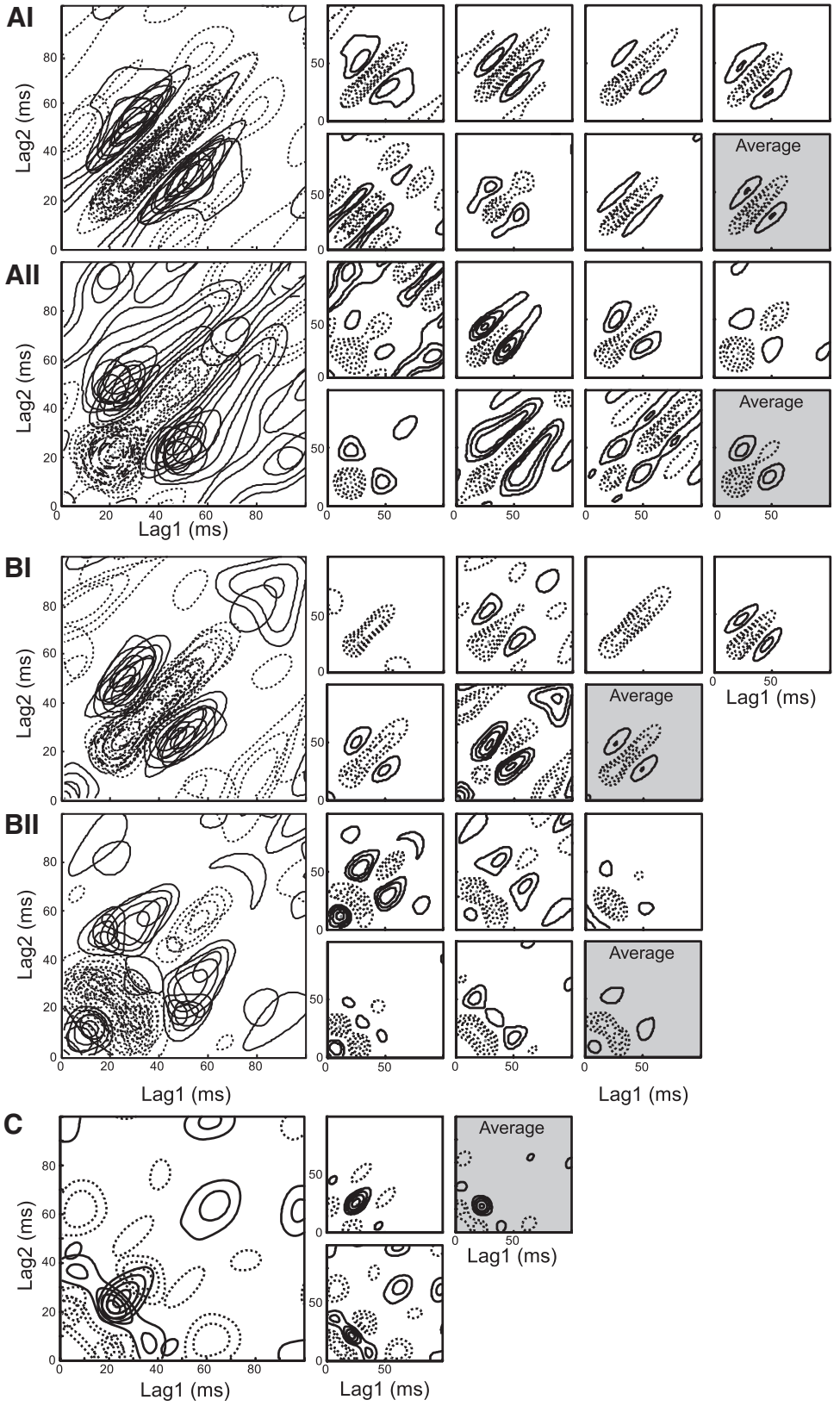

FIG. 5. The 2nd-order Wiener kernels of spiking local interneurons. Responses are shown for 27 of the 29 interneurons (see METHODS). *A*: the kernels from the interneurons in group 1 can be further divided into 2 subgroups. The 1st subgroup (*Ai*) had large τ_1 and τ_2, indicating a slower response time than the 2nd group (*Aii*). *B*: similarly the kernels of the interneurons in group 2 could also be divided into those with large (*Bi*) and small (*Bii*) τ_1 and τ_2. This trend was continued for the peaks of the kernels of the interneurons in group 3 (*C*). Interneurons belonging to the 1st and 2nd groups had dominant negative peaks, whereas interneurons in the 3rd group had dominant positive peaks. The interneurons in each group were not identical but had kernels along a spectrum that was continuous between the different groups. For each group, the large plot shows all the responses superimposed while the shaded plot shows the average.

neuron behaves in accordance with the model. The accuracy of the estimated models and the degree of linear and nonlinear components varied considerably (Fig. 7, *A–D*). For the linear models, the mean fitness of the 29 interneurons was 16.7 ± 2.18% (Fig. 7*A*); 43.7% was the highest fit obtained, and in more than half of the cases, the linear models predict <20% of the synaptic response. The nonlinear models had an average fit of 32.0 ± 2.3% and maximum of 55.5% with most models predicting between 20 and 50% of the response measured in the interneurons (see Fig. 7*C*).

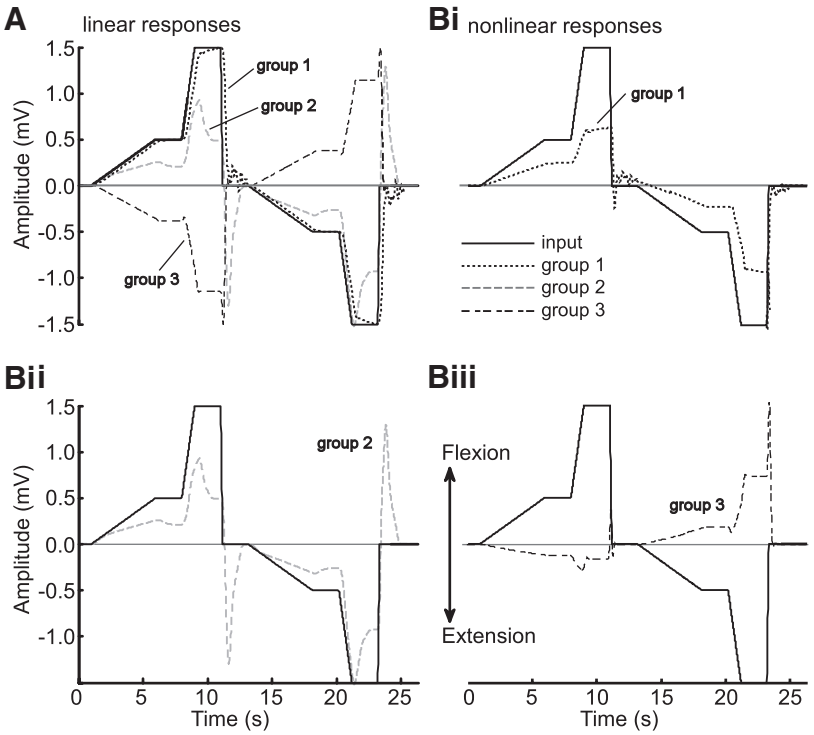

FIG. 6. Modeled responses of the interneurons. The output responses are normalized to the maximum magnitude of input signal. *A*: the linear responses of an interneuron taken from each group. *B*: nonlinear models, which are the sum of the 1st- and 2nd-order models. *I*: the position-sensitive neuron in group 1 closely followed the input signal in both flexion and extension directions with an inhibitory response during extension. *ii*: the interneuron in group 2 showed large values when the velocity was high and reduced responses during constant displacement. *iii*: the interneurons in group 3 were excited during extension and responded only weakly to flexion, and showed sustained, mainly position sensitive responses.

To assess the relative contributions made by the linear and nonlinear components of the model, we expressed the linear fit as a percentage of the total fit (Fig. 7*B*). We then classified interneurons as primarily linear if this percentage exceeded 50%. Thus 17 of the 29 interneurons modeled behaved "linearly." Visual analysis of the signals recorded in response to GWN stimulation showed that these (as expected) received both excitatory and inhibitory inputs (Fig. 7*D*). It should be emphasized that this visual inspection was carried out blind, i.e., without knowledge of the kernels for that recording. Of the remaining interneurons, 10 had predominantly nonlinear dynamics.

Comparing the predictive power of the models with the interneuron groups described earlier (Fig. 4) showed that interneurons receiving excitatory and inhibitory synaptic inputs belonged to group 1 (11 of 15), which are therefore more linear (while the others are more nonlinear, Fig. 7*D*). The model fit for interneurons receiving mixed inputs (22.9 ± 3.4%) and those receiving only inhibition (6.5 ± 2.1%, *t*-test: $t = -3.047$, $P = 0.011$) were significantly different.

Spiking local interneurons always showed spontaneous synaptic activity, even in the absence of FeCO stimulation, as recorded prior to the onset of GWN stimulation (for example see Fig. 3). It is therefore not surprising that during stimulation the model fit was mostly <50% indicating that less than half of the variance in the signal recorded from the interneuron could be predicted by the mathematical model and the mechanical input to the FeCO. In 20 of the 29 interneuron responses used, we had ≥2 s of baseline recording before or after the onset of stimulation. The power spectrum of this spontaneous activity was then compared with that of the residual of the model during stimulation (unexplained response, given by the difference between measured and predicted signal). The example in Fig. 7*E* shows that at frequencies below 30 Hz, the spontaneous synaptic activity prior to stimulation was of a similar level to that of the residual. At higher frequencies, the residual had lower power than the spontaneous activity. In this and other recordings, the synaptic noise (recording prior to stimulus onset) could account for ≤50% of the total synaptic response to FeCO stimulation. The rather low level of fitness observed (usually <50%) should therefore not be considered to indicate a poor choice of model, given the levels of spontaneous activity.

DISCUSSION

The neural circuitry responsible for controlling leg movement and reflexive pathways in the locust is among the best understood in any animal. Previous work has revealed the numbers and identities for most of the key components responsible for the generation of movement as well as the feedback loops necessary to maintain its adaptiveness (Berkowitz and Laurent 1996; Bräunig 1985; Bräunig and Eder 1998; Burrows 1982, 1987a,b, 1988; Burrows and Pflüger 1986; Field and Burrows 1982). Spiking local interneurons play an important role in reflex loops controlling the leg by integrating sensory information from the chordotonal organ and other sensory receptors and synapsing onto nonspiking local interneurons (Burrows 1987a), projection interneurons (Laurent 1987), and motor neurons (Burrows 1982).

The ventral midline population of spiking interneurons receive inputs from the FeCO and from leg exteroreceptors (Burrows 1988). During FeCO stimulation, information about tibial movement is encoded by these interneurons so that each receives inputs from a specific set of receptors (Burrows and Siegler 1982). Additionally, interneurons encode different properties of the stimuli with some coding for position and others for velocity or acceleration.

The use of the Wiener kernel method coupled with a GWN stimulus allowed us to characterize in detail a population of

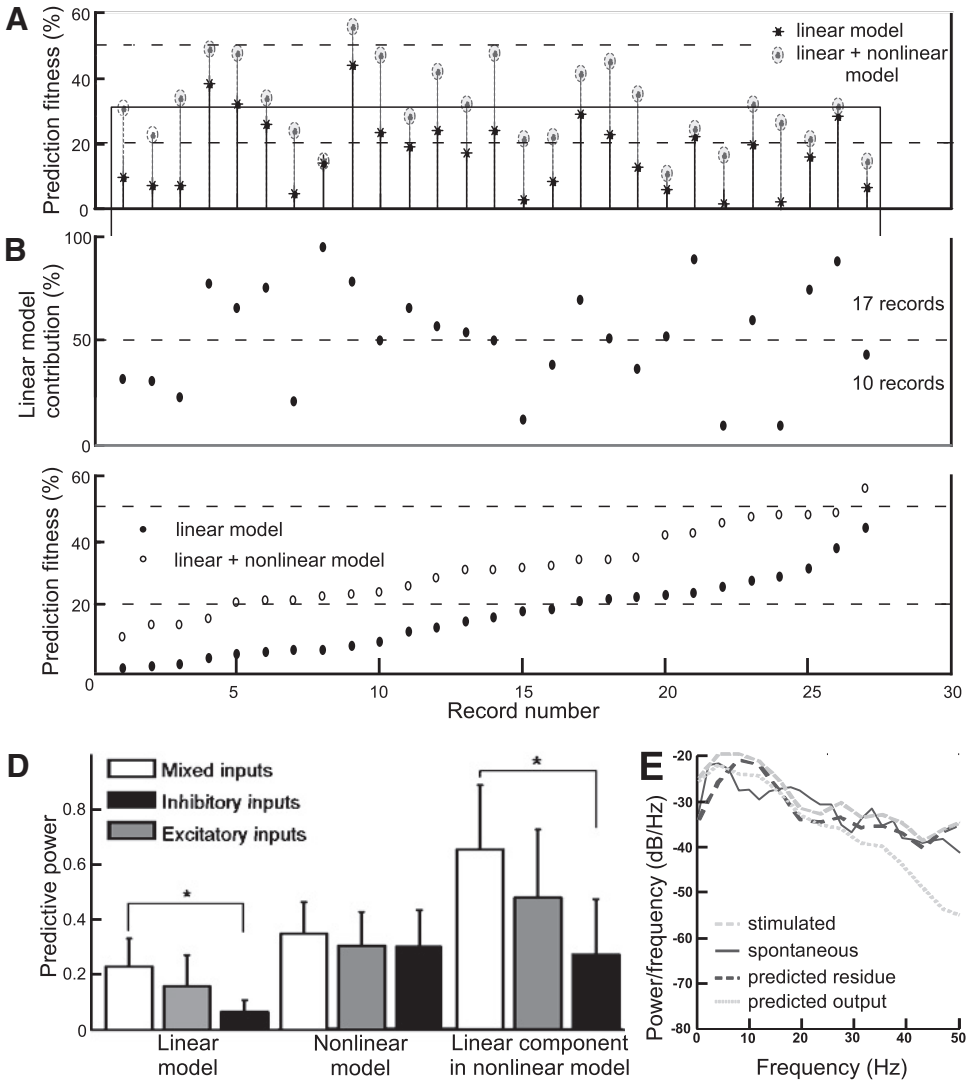

FIG. 7. Predictive power of linear and nonlinear models. The linear and nonlinear models used could predict ≤55% of the synaptic activity of the interneurons (*A*). The majority of the synaptic activity in these interneurons was not linear (*B*). Spiking local interneurons received a range of inputs and the degree to which their activity represented FeCO activation was graded with some interneurons having almost no correlation with mechanical stimulation and other ones having most of their synaptic activity dictated by FeCO inputs (*C*). Regardless of their correlation with FeCO activity, the nonlinear component of the interneurons synaptic activity contributed ~15–20% to their linear properties (*C*). Interneurons receiving both excitatory and inhibitory inputs behaved more linearly than those receiving only one type of input alone (*D*). The presence of spontaneous synaptic inputs is evident when comparing the power level curves before and during FeCO stimulation in one recording. Spontaneous inputs can account for ≤50% of the total output energy in this interneuron (*E*).

spiking interneurons known to play an important role in the production of reflex movements of the hind leg. The first- and second-order kernels were graded and overlapping, with a range of times to peak responses, suggest that spiking local interneurons use population coding to represent the sensory input they receive from the FeCO in the production of a resistance leg reflex.

Spiking local interneurons of the midline population

In a morphological study of the ventral midline population of spiking local interneurons, Siegler and Burrows (1984) found that there were ~100 somata of interneurones in each hemiganglion, although not all were spiking local interneurons as some had axons, whereas others were from nonspiking interneurons. Individual spiking local interneurons in this population receive synaptic inputs from proprioceptors only, from exteroceptors only, and convergently from both types of receptor (Burrows 1987). None have yet been identified as individuals; as Burrows (1985) highlighted it is not clear whether an interneuron is unique or whether it belongs to a small pool of interneurons with similar physiology and morphology. It is clear, however, that interneurons that receive proprioceptive inputs are morphologically distinct from those that receive exteroceptive inputs (Burrows 1987), however, no correlation has yet been made between morphology and coding properties of those that receive proprioceptive inputs. Burrows (1985, 1988) suggested that as few as 25% of the somata on the ventral midline are from spiking local interneurons that respond to leg movements about the femoro-tibial joint. Given that it is not clear if any of these interneurons are unique individuals, it is difficult to determine exactly what proportion of the interneuron pool receiving proprioceptive inputs have been encountered in our study. Sampling bias clearly cannot be ruled out as the somata range in diameter from 10 to 30 to μm (Siegler and Burrows (1985), however the large number of interneurons studied in detail, and which have similar linear properties to those described by Burrows (1988), suggest that the response properties of a large proportion of the interneurons known to receive proprioceptive inputs have been quantified in this study. It remains possible, however, that additional types may remain to be described. The results suggest that there is a continuous range of responses, which can, however, be roughly classified into three groups. This suggests that population coding is present to achieve a wider range of responses. While it is possible that there are neurons dealing

with specialist functions (e.g., corresponding to "safety receptors" responding to extreme extensions), we found no evidence for these. It could also be that more extreme (and specific) stimuli are required to elicit such specialized responses.

Coding characteristics of siking local interneurons

Interneurons responses were first classified into three groups by the K-means cluster analysis of the frequency responses (groups 1–3 in Fig. 4). These classifications were further reinforced according to physiological properties based on visual inspection of their recorded signals (also 3 clusters) and followed patterns of activity described in the locust by Burrows (1988) and stick insect by Büschges (1989). Interneurons were either excited, inhibited or received both excitation and inhibition during FeCO stimulation. Cluster 1 included 11 of the 15 interneurons in group 1, cluster 2 included 8 of the 10 in group 2, and cluster 3 all 4 interneurons in group 3. Moreover, the combined response of the first- and second-order kernels of groups 1 and 2 show dominant positive peaks in their first-order responses during extension and are therefore inhibited by extension. On the other hand group 3 interneurons had dominant negative peaks in the first-order kernels and positive peaks in the second-order kernels and were therefore excited by extension. The frequency response of the interneurons also further subdivided them into being mainly positions sensitive (having 0 slopes) and velocity sensitive (positive slopes). Finally the first- and second-order kernels of the interneurons fall within a continuum of graded peak responses times. Interneurons with similar linear responses have been described by Burrows (1988) and by Büschges (1989).

Our results suggests that all interneurons were either sensitive to extension or to both extension and flexion (no interneurons were found to solely respond to flexion), and most (25 of 29) showed an inhibitory response to tibial extension as was also found in stick insects (Büschges 1989). One possible explanation for this finding relates to the nature of the reflex in which the spiking interneurons participate as well as the way in which this joint is used in locomotion. During walking, the hindleg tibia is extended during the stance phase of the step (Burns 1973; Duch and Pflüger 1995) (while the tarsus is in ground contact), and because the tarsus is not moving with respect to the ground, the tibia is not likely to encounter an obstacle that might cause it to flex and trigger a resistance reflex. During the swing phase of the step (when the tarsus is off the ground), however, the tibia is actively flexed through the air and is more likely to encounter an obstacle that might cause it to extend and thus trigger a resistance reflex. Having more extension- than flexion-sensitive spiking interneurons could be a form of sensory tuning favoring the type of stimuli that the animal is more likely to encounter. For example, sideways-walking shore crabs rely heavily on chemotaxis and have sensory hairs concentrated on the lateral edges of their legs (which maximizes the chance of chemo-detection), in contrast with the nonlocalized distribution seen on the legs of forward-walking crustaceans (Vidal-Gadea et al. 2008). The dorsal setae of lobsters are yet another example where directionally sensitive structures are arranged so that they will face water flow while the animal is in its resting position (Vedel and Clarac 1976).

Population coding by spiking local interneurons

We found that the set of estimated kernels from the interneurons were similar in overall shape with response characteristics being graded along a spectrum, thus coding for different aspects of the stimulus. The kernels found in previous work on sensory neurons (Kondoh et al. 1995) showed a wider range of very distinct patterns (with a clearer distinction between position- and velocity-sensitive neurons) rather than being different by grades as observed in the present work. For the extensor motor neurons, on the other hand (Newland and Kondoh 1997b), first-order kernels are very consistent across recordings. The graded differences and overlapping patterns of kernels observed in the interneurons, and the finding that no interneuron was found to code solely for either position, velocity, or acceleration, suggest that the task of encoding the stimulus properties is distributed among the population of interneurons as a whole. It is therefore likely that movement of the tibia is encoded by the entire population of spiking local interneurons.

To our knowledge, this is the first description of a group of interneurons using population coding for sensory information in the production of reflex movement. These results could provide clues for elucidating sensory encoding mechanisms in vertebrate proprioceptive feedback where involuntary afterconstractions are modulated through yet unknown mechanisms (Adamson and McDonagh 2004). It is known that ankle movement is encoded by cutaneous afferents using population vectors, which combined with muscle spindle feedback produces stronger responses than either kind could alone (Aimonetti et al. 2007). Similar effects are found with spiking local interneurons produced by stimulating exteroreceptors and the FeCO simultaneously in the locust leg (Burrows and Siegler 1982), hinting at the importance of integrating multiple sensory modalities in the production of appropriate reflexes. One potential advantage of this integration could be the added safety obtained by having independent confirmation by two sensory structures before a potential maladaptive reflex is triggered (an ability sometimes considered to be a fundamental property of higher nervous systems) (Stein et al. 1989). For example, the resistance reflex mediated by the locust spiking local interneurons in response to FeCO activation is modulated by input to this population from exteroreceptors on the ventral tarsus so that the reflex will not occur while the leg is in ground contact (Burrows 1988). The range fractionation previously described for spiking local interneurons in locust (Burrows 1988) and stick insects (Büschges 1989) is likely to be a component of the coding properties of this population of interneurons where different interneurons respond to particular stimuli, aspects and ranges. As new techniques begin to allow the characterization of entire populations of neurons a picture emerges where behaviors are not the product of a linear chain of command but rather produced by the interaction among entire populations. This type of coding has already been shown to take place in the abdominal positioning system of the crayfish (Jellies and Larimer 1986; Larimer 1988), the escape circuit of crickets (Miller et al. 1991) and cockroaches (Camhi and Levy 1989), limb direction in monkeys (Georgopoulos 1991), and owl head movement in response to auditory cues to name only a few examples (Masino and Knudsen 1990).

Characterization of spiking local interneurons using mathematical modeling

The use of Wiener kernel analysis means that not only were we able to precisely quantify the linear and nonlinear responses to GWN inputs but that the methods produced robust mathematical models that were used to test an interneuron's response to any arbitrary input. The resulting models were able to predict ≤55% of the spiking local interneurons synaptic response to GWN stimulation of the FeCO. This accuracy is similar to that obtained for the flexor and extensor tibia motor neurons (Newland and Kondoh 1997a,b) and reflects the fact that these interneurons also receive a constant barrage of synaptic inputs from other sources besides the FeCO (Burrows 1982). In our work, we found that the power levels of spontaneous synaptic activity in the quiescent period before stimulation is similar to the power of the component of responses during stimulation that cannot be explained by the modeling. This indicates that the model performs as well as might reasonably be expected since it would have been surprising if the unexplained residual signal were smaller than ongoing spontaneous activity.

Interneurons that received mixed (excitatory and inhibitory) input behaved more linearly than those interneurons that received only one kind, which again was expected, because in order for a spiking local interneuron to behave linearly, it must be excited by imposed movement in one direction and inhibited by movement in the opposite direction. Approximately one-third of the interneurons recorded showed mixed inputs and for these the linear component of the model contributed the most to their output prediction.

Role of spiking local interneurons in reflexive pathway

Previous work on the connectivity of FeCO afferents revealed that during tibial extension, a subset of these excite flexor tibiae motor neurons as well as a subset of local spiking interneurons (Burrows 1987). The converse was also shown during tibial flexion with tibiae motor neurons and a different subset of local spiking interneurons being excited (Burrows 1987). Characterization of the dynamic properties of FeCO afferents (Kondoh et al. 1995), the two tibial extensors (Newland and Kondoh 1997b), and nine flexor motor neurons (Newland and Kondoh 1997a) showed similar population coding of tibial motion as that observed in the spiking local interneurons by flexor motor neurons but not by extensor motor neurons (including kernel shapes, times to peak, and the graded differences between different neurons observed in spiking interneurons). Since there are only two extensor motor neurons, and they are specialized for different tasks (SETi is used during walking) (see Burns and Usherwood 1979), one would not expect to find any kind of group operations being carried out by these neurons. However, the encoding carried out by the nine flexor motor neurons hints at the potential ubiquity of population coding even by small numbers of neurons in relatively simple tasks.

This Wiener kernel analysis of interneuron responses has allowed us to not only to characterize their response but also to model their response to any potential stimulus. This means that by knowing the joint excursion during a particular behavior (such as walking, scratching, or jumping), we are able to model the output of every interneuron in this population. This is an essential step to understand the production of reflexive limb movement in the locust and other systems and points to further work to characterize the responses of nonspiking local interneurons as they are responsible for controlling the activity patterns of groups of motor neurons.

GRANTS

This work was supported with awards from the Biotechnology and Biological Sciences Research Council (UK), and the Gerald Kerkut Charitable Trust (UK).

REFERENCES

Adamson G, McDonagh M. Human involuntary postural aftercontractions are strongly modulated by limb position. *Eur J Appl Physiol* 92: 343–351, 2004.

Aimonetti J-M, Hospod V, Roll J-P, Ribot-Ciscar E. Cutaneous afferents provide a neuronal population vector that encodes the orientation of human ankle movements. *J Physiol* 580: 649–658, 2007.

Aonuma H, Newland PL. Synaptic inputs onto spiking local interneurons in crayfish are depressed by nitric oxide. *J Neurobiol* 52: 144–155, 2002.

Bassler U. "Kniesehnenreflex" bei *Carausius morosus*: Ubergangsfunktion und Frequenzgang. *Kybernetik* 11: 32–50, 1972a.

Bassler U. Regelkreis des Kniesehnenreflex bei *Carausius morosus*: Reaktionen auf passive bewegungen der tibia. *Kybernetik* 12: 8–20, 1972b.

Bellazzi R, Larizza C, Magni P, Montani S, Stefanelli M. Intelligent analysis of clinical time series: an application in the diabetes mellitus domain. *Art Intel Med* 20: 37–57, 2000.

Berg RW, Alaburda A, Hounsgaard J. Balanced inhibition and excitation drive spike activity in spinal half-centers. *Science* 315: 390–393, 2007.

Berkowitz A. Broadly tuned spinal neurons for each form of fictive scratching in spinal turtles. *J Neurophysiol* 86: 1017–1025, 2001.

Berkowitz A. Spinal interneurons that are selectively activated during fictive flexion reflex. *J Neurosci* 27: 4634–4641, 2007.

Berkowitz A. Physiology and morphology of shared and specialized spinal interneurons for locomotion and scratching. *J Neurophysiol* 99: 2887–2901, 2008.

Berkowitz A, Laurent G. Local control of leg movements and motor patterns during grooming in locusts. *J Neurosci* 16: 8067–8078, 1996.

Boyd S, Chua LO. Fading memory and the problem of approximating nonlinear operators with Volterra series. *IEEE Trans Circuits Syst* 32: 1150–1161, 1985.

Bräunig P. Strand receptor associated with the femoral chordotonal organs of locust legs. *J Exp Biol* 116: 331–341, 1985.

Braünig P, Eder M. Locust dorsal unpaired median (DUM) neurones directly innervate and modulate hindleg proprioceptors. *J Exp Biol* 201: 3333–3338, 1998.

Briggman KL, Kristan Jr WB. Multifunctional pattern-generating circuits. *Annu Rev Neurosci* 31: 271–294, 2008.

Burns MD. The control of walking in *Orthoptera.* I. Leg movements in normal walking. *J Exp Biol* 58: 45–58, 1973.

Burns MD, Usherwood PNR. The control of walking in *Orthoptera.* II. Motor neuron activity in normal free-walking animals. *J Exp Biol* 79: 69–98, 1979.

Burrows M. The processiong of mechanosensory information by spiking local interneurons in the locust. *J Neurophysiol* 54: 463–478, 1985.

Burrows M. Inhibitory interactions between spiking and nonspiking local interneurons in the locust. *J Neurosci* 7: 3282–3292, 1987a.

Burrows M. Parallel processing of proprioceptive signals by spiking local interneurons and motor neurons in the locust. *J Neurosci* 7: 1064–1080, 1987b.

Burrows M. Responses of spiking local interneurons in the locust to proprioceptive signals from the femoral chordotonal organ. *J Comp Physiol [A]* 164: 207–217, 1988.

Burrows M, Horridge GA. The organization of inputs to motoneurons of the locust metathoracic leg. *Phil Trans R Soc Lond B Biol Sci* 269: 49–94, 1974.

Burrows M, Pflüger H-J. Processing by local interneurons of mechanosensory signals involved in a leg reflex of the locust. *J Neurosci* 6: 2764–2777, 1986.

Burrows M, Siegler MVS. Spiking local interneurones mediate local reflexes. *Science* 217: 650–652, 1982.

Büschges A. Processing of sensory input from the femoral chordotonal organ by spiking interneurons of the stick insect. *J Exp Biol* 144: 81–111, 1989.

Camhi JM, Levy A. The code for stimulus direction in a cell assembly in the cockroach. *J Comp Physiol [A]* 128: 193–201, 1989.

Coillot JP, Boistel J. Localisation et description des recepteurs a l'etirement au niveau de l'articulation tibio-femorale de la patte sauteuse du croquet, *Schsitocerca gregaria*. *J Insect Physiol* 14: 1661–1667, 1968.

Cordo PJ, Flores-Vieira C, Verschueren SMP, Inglis JT, Gurfinkel V. Position sensitivity of human muscle spindles: single afferent and population representations. *J Neurophysiol* 87: 1186–1195, 2002.

Daw CS, Finney CEA, Tracy ER. A review of symbolic analysis of experimental data. *Rev Sci Inst* 74: 915–925, 2003.

Duch C, Pflüger H-J. Motor patterns for horizontal and upside-down walking and vertical climbing in the locust. *J Exp Biol* 198: 1963–1976, 1995.

Field LH, Burrows M. Reflex effects of the femoral chordotonal organ upon leg motor neurones of the locust. *J Exp Biol* 101: 265–285, 1982.

Field LH, Rind FC. A single insect chordotonal organ mediates inter- and intra-segmental leg reflexes. *Comp Biochem Physiol* 68(A): 99–102, 1981.

Finlayson LH, Lowenstein O. The structure and function of abdominal stretch receptors in insects. *Proc Roy Soc Lond B Biol Sci* 148: 433–449, 1958.

Fischer H, Schmidt J, Haas R, Büschges A. Pattern generation for walking and searching movements of a stick insect leg. I. Coordination of motor activity. *J Neurophysiol* 85: 341–353, 2001.

French AS. Mechanotransduction. *Annu Rev Physiol* 54: 135–152, 1992.

Full RJ. Invertebrate locomotor systems. In: *The Handbook of Comparative Physiology*, edited by Dantzler W. Oxford, UK: Oxford Univ. Press, 1994, p. 853–930.

Georgopoulos AP. Neural coding of the direction of reaching and a comparison with saccadic eye movement. *Cold Spring Harb Symp Quant Biol* 55: 849–859, 1990.

Georgopoulos AP. Higher order motor control. *Annu Rev Neurosci* 14: 361–378, 1991.

Gordon J. Spinal mechanisms of motor coordination. In: *Principles of Neural Science*, edited by Kandel ER, Schwartz JH, Jessell TM. New York: Elsevier, 1991, p. 581–595.

Gordon J, Ghez C. Muscle receptors and spinal reflexes: the stretch reflex. In: *Principles of Neural Science*, edited by Kandel ER, Schwartz JH, Jessell TM. New York: Elsevier, 1991, p. 564–580.

Gordon IT, Whelan PJ. Deciphering the organization and modulation of spinal locomotor central pattern generators. *J Exp Biol* 209: 2007–2014, 2006.

Grillner S, Wallén P. Cellular bases of a vertebrate locomotor system—steering, intersegmental and segmental co-ordination and sensory control. *Brain Res Rev* 40: 92–106, 2002.

Hartigan JA, Wong MA. A K-means clustering algorithm. *Appl Stats* 28: 100–108, 1979.

Hilton WA. Afferent and efferent pathways in an abdominal segment of an insect. *J Comp Neurol* 36: 299–308, 1924.

Hinder MR, Milner TE. The case for an internal dynamics model versus equilibrium point control in human movement. *J Physiol* 549: 953–963, 2003.

Hultborn H. State-dependent modulation of sensory feedback. *J Physiol* 533: 5–13, 2001.

Ijspeert AI. Locomotion, vertebrate. In: *The Handbook of Brain Theory and Neural Networks* (2nd ed). MIT Press, 2002, p. 649–654.

Jellies J, Larimer JL. Activity of crayfish abdominal-positioning interneurons during spontaneous and sensory-evoked movements. *J Exp Biol* 120: 173–188, 1985.

Jing XJ. *Frequency Domain Theory of Nonlinear Volterra Systems Based on Parametric Characteristic Analysis* (PhD thesis). University of Sheffield, UK, 2008.

Jing XJ, Lang ZQ, Billings SA. Output frequency response function based analysis for nonlinear Volterra systems. *Mech Syst Sig Process* 22: 102–120, 2008.

Kargo WJ, Giszter SF. Afferent roles in hindlimb wipe-reflex trajectories: free-limb kinematics and motor patterns. *J Neurophysiol* 83: 1480–1501, 2000.

Kondoh Y, Okuma J, Newland PL. Dynamics on neurons controlling movement of a locust hind leg: Wierner Kernel analysis of the responses of proprioceptive afferents. *J Neurophysiol* 73: 1829–1842, 1995.

Kristan WB Jr, Shaw BK. Population coding and behavioural choice. *Curr Opin Neurobiol* 7: 826–831, 1997.

Larimer JL. The command hypothesis: a new view using an old example. *Trends Neurosci* 11: 506–510, 1988.

Laurent G. The role of spiking local interneurons in shaping the receptive fields of intersegmental interneurons in the locust. *J Neurosci* 7: 1977–1989, 1987.

Lee YW, Schetzen M. Measurement of theWiener kernels of a nonlinear system by cross-correlation. *Int J Control* 2: 237–254, 1965.

Marmarelis PZ. *Nonlinear Dynamic Modeling of Physiological Systems.* New York: Wiley, 2004.

Marmarelis PZ, Marmarelis VZ. *Analysis of Physiological Systems.* New York: Plenum, 1978.

Marmarelis PZ, Naka K-I. White noise analysis of a neuron chain: an application of the Wiener theory. *Science* 175: 1276–1278, 1972.

Masino T, Knudsen EI. Horizontal and vertical components of head movement are controlled by distinct neural circuits in the barn owl. *Nature* 345: 434–437, 1990.

Matheson T, Field LH. Innervation of the metathoracic femoral chordotonal organ of *Locusta migratoria. Cell Tissue Res* 259: 551–560, 1990.

Matthews BHC. Nerve endings in mammalian muscle. *J Physiol* 78: 1–53, 1933.

Mathews PBC, Stein RB. The sensitivity of muscle spindle afferents to small sinusoidal changes in length. *J Physiol* 200: 723–743, 1969.

Maynard EM, Hatsopoulus NG, Ojakangas CL, Acuna BD, Sanes JN, Normann RA, Donoghue JP. Neuronal interactions improve cortical population coding of movement direction. *J Neurosci* 19: 8083–8093, 1999.

Miller JP, Jacobs GA, Theunissen FE. Representation of sensory information in the cricket cercal sensory system. I. Response properties of the primary interneurons. *J Neurophysiol* 66: 1680–1689, 1991.

Morasso P. Spatial control of arm movement. *Exp Brain Res* 42: 223–227, 1981.

Newland PL. Processing of gustatory information by spiking local interneurons in the locust. *J Neurophysiol* 82: 3149–3159, 1999.

Newland PL, Kondoh Y. Dynamics of neurons controlling movement of a locust hind leg. II. Flexor tibiae motor neurons. *J Neurophysiol* 77: 1731–1746, 1997a.

Newland PL, Kondoh Y. Dynamics of neurons controlling movement of a locust hind leg. III. Extensor tibiae motor neurons. *J Neurophysiol* 77: 3297–3310, 1997b.

Pearson KG. Common principles of motor control in vertebrates and invertebrates. *Annu Rev Neurosci* 16: 265–297, 1993.

Pringle JWS. Proprioception in insects. I. A new type of mechanical receptor from the palps of the cockroach. *J Exp Biol* 15: 101–113, 1938a.

Pringle JWS. Proprioception in insects. II. The action of the campaniform sensilla on the legs. *J Exp Biol* 15: 114–131, 1938b.

Rogosina M. Uber das perisphere Nervensystem der *Aeschna*-Larve. *Z Zellfisch* 6: 732–758, 1928.

Rybak IA, Ivashko DG, Prilutsky BI, Lewis MA, Chapin JK. Modeling neural control of locomotion: integration of reflex circuits with CPG. *Proc Int Conf Artificial Neural Networks* 15: 99–104, 2002.

Sakuranaga M, Naka KI. Signal transmission in the catfish retina. V. Sensitivity and circuit. *J Neurophsiol* 58: 1329–1350, 1987.

Schetzen M. Nonlinear system modeling based on the Wiener theory. *Proc IEEE* 69: 1557–1573, 1981.

Schultz RA, Miller DC, Kerr CS. Mechanoreceptors in human cruciate ligaments. *J Bone Joint Surg* 66: 1072–1076, 1984.

Scott SH. Optimal feedback control and the neural basis of volitional motor control. *Nat Rev Neurosci* 5: 532–546, 2004.

Siegler MVS, Burrows M. The morphology of two groups of spiking local interneurons in the metathoracic ganglion of the locust. *J Comp Neurol* 224: 463–482, 1984.

Silvering AF, Okada R, Ito K, Galizia CG. Olfactory information processing in the *Drosophila* antennal lobe: anything goes? *J Neurosci* 28: 13075–13087, 2008.

Sinclair D. *Mechanisms of Cutaneous Sensation.* Oxford, UK: Oxford Univ. Press, 1981.

Slifer EH, Finlayson LH. Muscle receptor organs in grasshoppers and locusts (*Orthoptera, Acrididae*). *Quart J Micr Sci* 97: 617–620, 1956.

St-Onge N, Adamovich SV, Feldman AG. Control processes underlying elbow flexion may be independent of kinematic and electromyographic patterns: experimental study and modeling. *Neurosci* 79: 295–316, 1997.

Stein BE, Meredith MA, Huneycutt WS, McDade L. Behavioral indices of multisensory integration: orientation to visual cues is affected by auditory stimuli. *J Cog Neurosci* 1: 12–24, 1989.

Stein W, Straub O, Ausborn J, Mader W, Wolf H. Motor pattern selection by combinatorial code of interneuronal pathways. *J Comp Neurosci* 25: 543–561, 2008.

Tresch MC, Saltiel P, d'Avella A, Bizzi E. Coordination and localization in spinal motor systems. *Brain Res Rev* 40: 66–79, 2002.

Tschuluun N, Hall WM, Mulloney B. Limb movement during locomotion: Test of a model of an intersegmental circuit. *J Neurosci* 21: 7859–7869, 2001.

Usherwood PNR, Runion HI, Campbell JI. Structure and physiology of a chordotonal organ in the locust leg. *J Exp Biol* 48: 305–323, 1968.

Vedel JP, Clarac F. Hydrodynamic sensitivity by cuticular organs in the rock lobster *Panulirus vulgaris.* Morphological and physiological aspects. *Mar Beh Physiol* 3: 235–251, 1976.

Vidal-Gadea AG, Rinehart MD, Belanger JH. Skeletal adaptations for forwards and sidewalks walking in three species of decapod crustaceans. *Arthropod Struct Dev* 37: 95–108, 1980.

Wang W, Chan SS, Heldman DA, Moran DW. Motor cortical representation of position and velocity during reaching. *J Neurophysiol* 97: 4258–4270, 2007.

Watson AHD, Burrows M. Immunocytochemical and pharmacological evidence for GABAergic spiking local interneurons in the locust. *J Neurosci* 7: 1741–1751, 1987.

Yanai Y, Adamit N, Israel Z, Harel R, Prut Y. Coordinate transformation is first completed downstream of primary motor cortex. *J Neurosci* 28: 1728–1732, 2008.

Zehr EP, Duysens J. Regulation of arm and leg movement during human locomotion. *Neuroscientist* 10: 347–361, 2004.

Zill SN, Moran DT. The exoskeleton and insect proprioception. I. Responses of tibial campaniform sensilla to external and muscle-generated forces in the American cockroach, *Periplaneta americana. J Exp Biol* 91:1–24, 1981.